

RSC Advances



This is an *Accepted Manuscript*, which has been through the Royal Society of Chemistry peer review process and has been accepted for publication.

Accepted Manuscripts are published online shortly after acceptance, before technical editing, formatting and proof reading. Using this free service, authors can make their results available to the community, in citable form, before we publish the edited article. This *Accepted Manuscript* will be replaced by the edited, formatted and paginated article as soon as this is available.

You can find more information about *Accepted Manuscripts* in the [Information for Authors](#).

Please note that technical editing may introduce minor changes to the text and/or graphics, which may alter content. The journal's standard [Terms & Conditions](#) and the [Ethical guidelines](#) still apply. In no event shall the Royal Society of Chemistry be held responsible for any errors or omissions in this *Accepted Manuscript* or any consequences arising from the use of any information it contains.

ARTICLE

A ZIF-8-based Platform for Rapid and Highly Sensitive Detection of Indoor Formaldehyde

Cite this: DOI: 10.1039/x0xx00000x

Huimin Zhao*, Xiaojing Li, Wanze Li, Peng Wang, Shuo Chen, Xie Quan

Received 00th January 2012,

Accepted 00th January 2012

DOI: 10.1039/x0xx00000x

www.rsc.org/

A rapid and highly sensitive sensor which can quantitatively detect indoor gaseous formaldehyde in 5 min based on Zeolitic Imidazolate Framework-8 (ZIF-8) is presented. ZIF-8 was synthesized by nontoxic zinc ions and 2-methylimidazole in aqueous solution at room temperature. The morphology, microstructure, stability and photoluminescence property of the material were characterized by scanning electron microscopy, nitrogen adsorption-desorption, X-ray diffraction, thermo gravimetric analysis and fluorometric analysis techniques, respectively. The results showed that the obtained material with a uniform particle size possessed of excellent thermal, structural stability and good luminescent property. Under the optimized condition, the photoluminescent intensity of the guest-free phase ZIF-8 was linear with the formaldehyde concentration in two intervals, 0-0.5 ppm and 0.5-20 ppm, with the correlative coefficients of 0.9991 and 0.9819, respectively. The limit of detection for gaseous formaldehyde was calculated to be 0.057 ppm ($3\delta/\text{slope}$ criterion). Moreover, other indoor pollutants emitted from indoor decorative materials, such as benzene, toluene, methanol and ethanol, showed little interference with the photoluminescence intensity of this platform during its determination process. The material exhibits great potential in the field of rapid, convenient and highly sensitive detection of indoor gaseous formaldehyde.

1. Introduction

Formaldehyde (HCHO), which is widely used in building and decorative industry as an additive in plywood, laminated wood board, chipboard and other building materials, can lead to seriously intense irritant of the eyes and mucous membranes.¹ Recent years, with the development of decoration housing, formaldehyde discharged from the chemical or thermal decomposition of building materials, gradually turns to be a highly problematic indoor pollutant.²⁻⁴ Due to its acute toxicity and volatility, Occupational Safety and Health Act (OSHA) has set the immediately dangerous to life or health limit (IDLH) and the permissible exposure limit (PEL) at 750 ppb and 20 ppm, respectively; For comparison, the World Health Organization (WHO) has set a safe-exposure standard of 80 ppb averaged over 30 min.⁵⁻⁶ However, conventional formaldehyde detecting methods are generally time-consuming (at least 30 min for sampling),⁷ and require costly instrumentation and skilled personnel, which cannot meet the requirements of routine detection and early warning. Therefore, it is critical to develop a rapid, simple and highly sensitive method for indoor formaldehyde detection.

Metal-organic Frameworks (MOFs) are a series of inorganic-organic hybrid materials, which are composed by two components, single metal ions or poly nuclear metal clusters and organic ligands usually coordinated through bonds.⁸⁻¹¹ Because of the interior interaction of host frameworks with specific guest analyte, the structural rigidity of MOFs is enhanced, which causes changes in photo-, electrochemical or other properties in the host framework. Therefore, it is possible to furnish a specific detection as fluorescent sensors offering an opportunity for practical application with a facile signal transduction. Over the past few years, a wide range of luminescent MOFs were widely developed for realizing sensing of cations,¹² anions,¹³ small molecules,¹⁴ vapors¹⁵ and a few of gases.¹⁶⁻¹⁷ Among them, recently, Ln-MOFs and Cu(I)-MOF are reported to be used as sensors for formaldehyde detection,¹⁸⁻¹⁹ exhibiting a high sensitivity for formaldehyde solution and formaldehyde vapor, respectively. However, these reported methods based on Ln-MOFs and Cu(I)-MOF are still time-consuming, especially for formaldehyde detection with low concentration. For example, it takes at least 4 h ~ 12 h for 0.016 ppm formaldehyde vapor detection.¹⁹

Motivated by our interest in this field, in this contribution, we demonstrate a rapid and highly sensitive sensor for detecting formaldehyde gas based on a luminescent ZIF-8 (Zeolitic Imidazolate Framework-8), which has the formula $\text{Zn}(\text{2-methylimidazole})_2$ with a sodalite-related zeolite type structure containing narrow six-membered-ring pore windows (3.4 Å) and much larger pores (11.4 Å).²⁰⁻²² In light of the excellent luminescent merits of ZIF-8 combining its porous features, as well as the relatively environmentally friendly and nontoxic nature of Zn^{II} to human health, it was selected to be an anticipated candidate for gaseous formaldehyde detection.

Herein, we investigated the feasibility and performance of ZIF-8 in formaldehyde sensitive detection. The photoluminescence (PL) properties of ZIF-8 before and after exposure to formaldehyde in the absence and presence of interferents (benzene, toluene, methanol and ethanol) were also conducted to evaluate its selectivity for indoor formaldehyde detection. And based on the changes of its PL properties, its sensing mechanism was discussed. To the best of our knowledge, there has been rare report published so far regarding the fast and sensitive detection of indoor formaldehyde based on MOFs.

2. Experiments

2.1. Materials and Methods

All chemicals including $\text{Zn}(\text{NO}_3)_2 \cdot 6\text{H}_2\text{O}$ (99%), 2-methylimidazole (98%), formaldehyde solution (37%~40%), methanol solution ($\geq 99.5\%$), ethanol solution ($\geq 99.5\%$), benzene solution ($\geq 99.5\%$) and toluene solution ($\geq 99.5\%$) were obtained from Guangfu Fine Chemicals, Tianjin, China, which were at least of analytical grade and were used without further purification. A certified, premixed formaldehyde tank and an air tank were obtained from Zhonghao Guangming Research & Design Institute of Chemical Industry Corporation located in Dalian, China. Gas streams containing low levels of formaldehyde were prepared by mixing the formaldehyde gas with air.

2.2. Synthesis of ZIF-8(a) and ZIF-8(b) particles

ZIF-8(a) nanocrystals (marked as ZIF-8(a) for simplification) were synthesized according to the literature of Shunsuke Tanaka et al.²³ Nanocrystals were obtained by the reaction of $\text{Zn}(\text{NO}_3)_2 \cdot 6\text{H}_2\text{O}$ and 2-methylimidazole in pure water. Briefly, 10 mL $\text{Zn}(\text{NO}_3)_2 \cdot 6\text{H}_2\text{O}$ solution (74.4 g/L) was added into 90 mL imidazole derivative (2-methylimidazole) solution (137 g/L) at room temperature. The mixture, which immediately turned into turbid liquid, was stirred with a magnetic bar for 24 h, then the milky colloidal dispersion was centrifuged at 6000 rpm for 10 min. The depositing particles washed by methanol for three times were dried at 40 °C for 48 h. Then ZIF-8(a) was obtained.

ZIF-8(b) nanocrystals (ZIF-8(a) after evacuation, denoted as ZIF-8(b)) were obtained by being evacuated at 150 °C in vacuum for 24 h.

2.3. Instruments

Morphologies of samples were observed using an S-4800 field emission scanning electron microscope (SEM, Hitachi Co., Japan). The relative elemental contents of samples were analyzed by energy dispersive X-ray spectroscopy (EDS) performed on the same instrument. The structural stability of crystal samples were investigated by X-ray diffractometer (XRD, EMPYREAN, PANalytical) between 5° and 50°. The purity and homogeneity of the products were determined by comparison between the simulated and experimental XRD patterns. The thermal stability of crystal samples were analyzed by thermal gravimetric analyzer (TGA/DTA, 6300, Seiko) from room temperature (about 25 °C) to 800 °C at a ramp rate of 10 °C/min under a nitrogen atmosphere and DSC analyzer (DSC, 910S, TA Instruments) from 50 °C to 400 °C. The surface functional groups and adsorbing behavior of the guest-free phase ZIF-8(b) were detected by a Fourier transform infrared spectrophotometer (FT-IR, VERTEX 70, Bruker) with KBr as the reference sample at 400-4000 cm^{-1} region. The N_2 adsorption-desorption property and total pore volume of samples were conducted by an Automated Surface Area and Pore size Analyzer (Quantachrome Autosorb-1 MP, American). PL intensities of the samples were measured using a fluorescence spectrometer (Hitachi F-4500, Japan).

2.4. Formaldehyde detection

The gas flow process was shown in Fig. 1. ZIF-8(b) was used as the sensor probe. Different concentrations of formaldehyde gas, which were achieved by the regulation of MFC (mass flow controller) to the desired formaldehyde concentration from 0 ppm to 20 ppm, flowed through ZIF-8(b) on the gas shelf. Then ZIF-8 was collected for further PL intensity analysis. To determine the optimized exposure time of formaldehyde to the guest-free phase ZIF-8(b), a series of time (0 min, 1 min, 2 min,

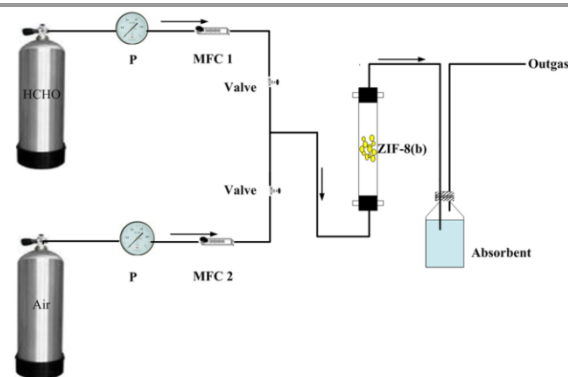


Fig. 1 The schematic of the gas flow during the formaldehyde detection based on ZIF-8 at room temperature. P stands for pressure gage. MFC = mass flow controller.

5 min, 10 min, 20 min, 30 min, 40 min, 50 min and 60 min) was selected.

2.5. Selectivity of ZIF-8-platform for formaldehyde detection

To evaluate the selectivity of ZIF-8 for formaldehyde detection, benzene, toluene, methanol and ethanol vapor with a concentration of 2 ppm were chosen as the interfering substances. Considering the feasibility to obtain various vapors under similar condition, the formaldehyde vapor and interfering substances vapor were performed by heating (~75 °C) the corresponding solution in a sealed vial (500 mL), respectively.¹⁹

In order to get the presumptive concentration of vapor, the various vapors were prepared according to the following equation, and the detailed results were listed in Tab. 1.

$$C = \omega\rho V/V_0$$

Where, C, the concentration of formaldehyde or interferent (ppm); ω , mass fraction of formaldehyde or interferent solution; ρ , density of formaldehyde or interferent solution (g/cm^3); V, volume of formaldehyde or interferent solution (μL); V_0 , vial volume (mL).

Tab. 1. The calculated parameters for preparation of formaldehyde and different interferents (2 ppm) by heating (~75 °C) the corresponding solution in a sealed vial (500 mL)

Substance	Mass fraction of solution, ω	Density of solution (g/cm^3), ρ	Volume of solution (μL), V	Vial volume (mL), V_0	Concentration (ppm), C
HCHO	20%	1	5	500	2
benzene	99.5%	0.88	1.1	500	2
toluene	99.5%	0.87	1.1	500	2
methanol	99.5%	0.79	1.3	500	2
ethanol	99.5%	0.79	1.3	500	2

2.6. Photoluminescence measurement

The PL properties of as-synthesized ZIF-8(a) and guest-free phase ZIF-8(b) after exposure to air or formaldehyde at room temperature were surveyed by a fluorescence spectrometer (Hitachi F-4500) with the scan speed of 1200 nm/min, response at 0.5 s and PMT voltage of 700 V. A Xenon lamp was used as the excitation source of the fluorescence spectrometer. The width of the excitation slit and the emission slit was 1 nm and 2.5 nm, respectively. The photoluminescence emission spectrum was recorded in the wavelength range of 360 - 690 nm upon excitation at 350 nm. The PL properties of ZIF-8(b) exposed to different concentrations of formaldehyde were investigated as well excited at 350 nm to obtain the detection range. The emission intensities of ZIF-8(b) after exposure to formaldehyde vapor in the absence and presence of different interfering gas (methanol, ethanol, benzene and toluene) were recorded at 350 nm excitation wavelength to illustrate the selectivity of ZIF-8 for formaldehyde detection.

3. Results and Discussion

3.1. Characterization of ZIF-8

The morphologies of the as-synthesized sample ZIF-8(a) and guest-free phase ZIF-8(b) characterized by SEM were presented in Fig. 2a and 2b. The size of the as-synthesized sample ZIF-8(a) crystals is almost 250 nm. Compared Fig. 2a with Fig. 2b, it is clearly that the morphology of sharp hexagonal facets was still maintained, demonstrating the good thermal stability of ZIF-8 after being evacuated at 150 °C in vacuum for 24 h. To further investigate the structural stability and adsorption capacity of as-synthesized materials at room temperature, XRD, TGA-DTA, DSC and N_2 adsorption-desorption isotherm were analyzed. XRD pattern of the as-synthesized sample ZIF-8(a) and guest-free phase ZIF-8(b) was almost equal to the simulated data calculated using Mercury 3.3, further indicated that ZIF-8(b) maintained a 3D structure after evacuated at 150 °C in vacuum for 24 h, as shown in Fig. 2c. Moreover, Both the DTA curve and the DSC curve presented an endothermic region at the temperature range of 50~250 °C, corresponding to the large mass loss in TGA curve, which was attributed to desorption of solvents (CH_3OH and H_2O) from the powder. From these figures, it is obvious that ZIF-8 is very stable lower than 500 °C (Fig. 2d and Fig. S1). Remarkably, the TGA curve was nearly similar to ZIF-8 synthesized by solvothermal method, illustrating the method used in this manuscript is feasible.²⁰ Furthermore, the N_2 adsorption-desorption property of ZIF-8(a) was also investigated. As depicted in Fig. 2e, ZIF-8(a) was found to exhibit type I isotherm characteristic of N_2 adsorption at 77 K with a BET (Brunner-Emmet-Teller) surface area of 731 m^2/g , the total pore volume is calculated to be 0.48 cm^3/g by DFT calculation method, which indicated its microporous characteristics and the data was comparative with those of ZIF-8 synthesized in aqueous solutions at room temperature.²⁴⁻²⁵ The different relative elemental contents of ZIF-8(a) and ZIF-8(b) were shown in Table. S1 and Table. S2. Compared to ZIF-8(a), the relative contents of C and O in ZIF-8(b) was obviously decreased, indicating the removal of solvent (CH_3OH and H_2O) after the treatment at 150 °C in vacuum for 24 h, which was similar to the data in TGA-DTA curve. And after the treatment, ZIF-8(b) was more active for formaldehyde detection.

3.2. Optimization of exposure time for formaldehyde detection

In order to study the potential of ZIF-8(b) for detecting of formaldehyde, PL intensity of the ZIF-8(b) after exposure to formaldehyde was evaluated with emission spectra. Owing to different time exposure to formaldehyde stands for various reacting dose, which will lead to dramatically change of PL emission intensity for sensing material, the exposure time of ZIF-8(b) to formaldehyde was chosen as a key factor. To determine the optimized accumulation time of the guest-free phase ZIF-8(b) exposed to formaldehyde, a series of time (0

min, 1 min, 2 min, 5 min, 10 min, 20 min, 30 min, 40 min, 50 min and 60 min) were selected. After exposure to 20 ppm (IDLH) formaldehyde gas in various time, the PL emission intensity of ZIF-8(b) was investigated. As shown in Fig. 3, after 1 min exposure to 20 ppm formaldehyde gas through the gas shelf under ambient pressure, the PL emission intensity of ZIF-

8(b) at 410 nm increased by about 7.8%. And up to 5 min, the PL emission intensity of ZIF-8(b) at 410 nm increased linearly with the exposure time, obtaining approximate 34.6% signal enhancement during the first 5 min. Then the PL emission intensity at 410 nm gradually kept a constant within the exposure of approximately 1 h. Hence, 5 min was selected as the optimized accumulation time for formaldehyde detection based on the guest-free phase ZIF-8(b).

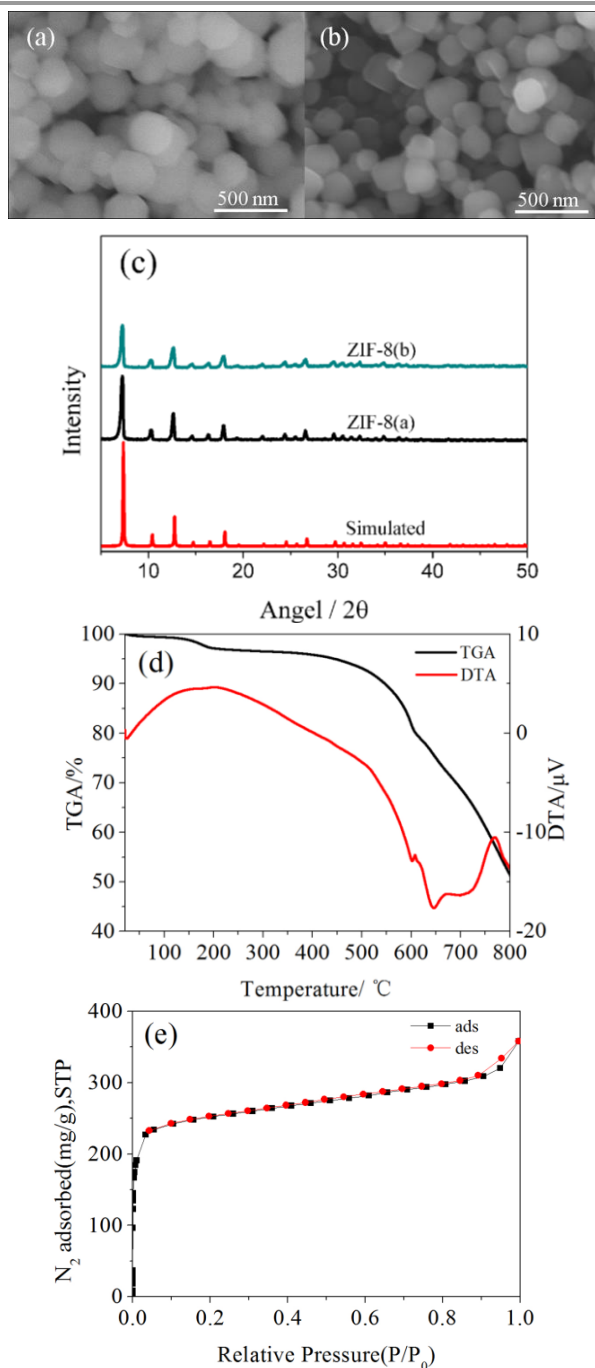


Fig. 2 (a) SEM images for as-synthesized sample ZIF-8(a). (b) SEM images for the guest-free phase sample ZIF-8(b) (the as-synthesized sample after treatment at 150 °C in vacuum for 24 h). (c) The XRD patterns of ZIF-8(a), ZIF-8(b) and the simulated one.²⁰ (d) TGA-DTA curve of the as-synthesized samples ZIF-8(a). (e) Nitrogen sorption isotherms of as-synthesized samples ZIF-8(a) nanocrystals at 77 K.

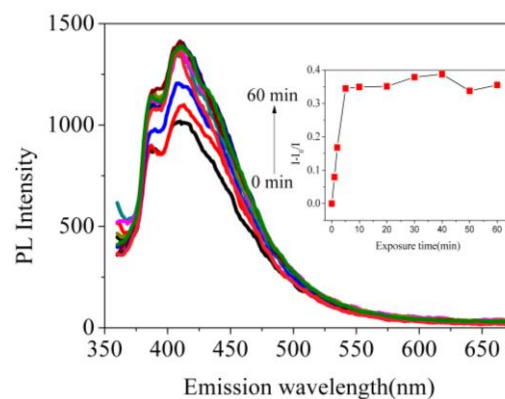


Fig. 3 Solid-state photoluminescence emission spectra of ZIF-8(b) after exposure to 20 ppm formaldehyde in various time (0 min, 1 min, 2 min, 5 min, 10 min, 20 min, 30 min, 40 min, 50 min and 60 min). $\lambda_{\text{ex}} = 350$ nm. Inset: Variations in PL intensity of ZIF-8(b) increase over time after exposure to 20 ppm formaldehyde. The PL intensity of the guest-free phase ZIF-8(b) was defined as I_0 , and I was the PL intensity of the guest-free phase ZIF-8(b) after exposure to 20 ppm formaldehyde in various time. $\lambda_{\text{ex}} = 350$ nm, $\lambda_{\text{em}} = 410$ nm.

3.3. Photoluminescence detection of formaldehyde

Under the optimized exposure time, the linear response range and the detection limit of the ZIF-8-based sensing system were measured as follows. The PL emission intensity at 410 nm of ZIF-8(b) after exposure to a group of formaldehyde concentrations (20 ppm, 15 ppm, 10 ppm, 5 ppm, 1 ppm, 500 ppb, 250 ppb, 100 ppb and 0 ppb) was investigated to evaluate the sensitivity of the ZIF-8-based sensing platform. As shown in Fig. 4, after exposure to formaldehyde gas for 5 min, different concentrations of formaldehyde induced distinct “turn-on” effect on PL intensity at 410 nm of the guest-free phase ZIF-8(b). From 0 ppb to 20 ppm, with the increase of formaldehyde concentration, the PL intensity of ZIF-8(b) at 410 nm was enhanced gradually. Moreover, the PL intensity of the guest-free phase ZIF-8(b) was linear with the formaldehyde concentrations in two intervals, 0 - 0.5 ppm and 0.5 - 20 ppm, with the correlative coefficients of 0.9991 and 0.9819, respectively. Based on $3\delta/\text{slope}$ criterion (δ , standard deviation of the blank samples), the limit of detection (LOD) was calculated to be 0.057 ppm, which is satisfied with the requirements of indoor danger threshold set by OSHA and safe-exposure standard set by WHO. Compared with other methods, for example, the reported methods based on Ln-MOFs or Cu(I)-MOF, this method based on ZIF-8 could result in a satisfactory detection limit and sensitivity for formaldehyde fast detection.

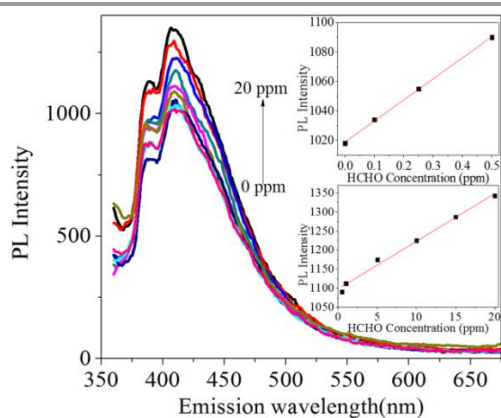


Fig. 4 Variations in solid-state photoluminescence emission spectra of ZIF-8(b) after exposure to different concentrations of formaldehyde for 5 min (0 ppb, 100 ppb, 250 ppb, 500 ppb, 1 ppm, 5 ppm, 10 ppm, 15 ppm and 20 ppm). $\lambda_{\text{ex}} = 350$ nm. Inset figure: two fitting lines for the emission intensity of ZIF-8(b) increased after exposure to different concentration of formaldehyde from 0 ppb to 20 ppm (upper one: 0 - 0.5 ppm, lower one: 0.5 - 20 ppm). $\lambda_{\text{ex}} = 350$ nm, $\lambda_{\text{em}} = 410$ nm.

3.4. Reversibility

Besides high sensitivity and low detection limit, reversibility is another crucial factor to assess the performance of sensor. To study the reversibility of ZIF-8-based sensing platform, the synthesized ZIF-8(b) after exposure to 20 ppm of formaldehyde was regenerated in vacuum at 150 °C for 24 h. Noticeably, the PL emission intensity of ZIF-8(b) could be regenerated completely (Fig. 5). And it was worth mentioned that the PL emission intensity at 410 nm maintained its original intensity even after several cycles of exposure to formaldehyde and vacuum treatment at 150 °C (Fig. 5). In Fig. S2, the morphology and XRD peaks of ZIF-8(b) in vacuum at 150 °C for 24 h regenerated had no change compared with ZIF-8(b) before adsorption formaldehyde, which demonstrates the stability of the structure. Because of the reversibility of ZIF-8(b) reused as the platform for formaldehyde fast detection, this results illustrated the feasibility and economic characteristics of this method.

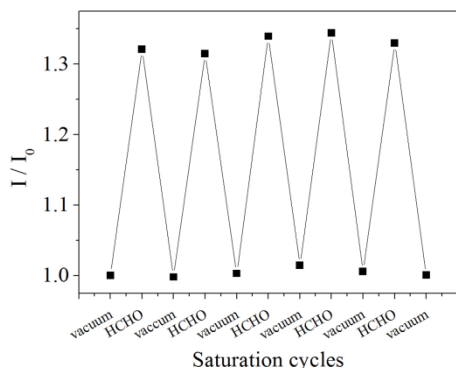


Fig. 5 Variations in PL Intensities of ZIF-8(b) over multiple cycles of exposure to 20 ppm formaldehyde and treatment in vacuum for 24 h at 150 °C. The PL intensity of the guest-free phase ZIF-8(b) was defined as I_0 , and I was the PL intensity of the guest-free phase ZIF-8(b) after exposure to 20 ppm formaldehyde or treatment in vacuum at saturation cycles. $\lambda_{\text{ex}} = 350$ nm, $\lambda_{\text{em}} = 410$ nm.

3.5. Selectivity

Whether there are false positive or negative effect caused by interferent substances is another key factor to evaluate the feasibility of the formaldehyde detection method. For many indoor formaldehyde detection methods, errors caused by indoor interferents emitting from indoor emission materials (such as furniture and building materials) inhibited the accurate detection of indoor formaldehyde. To evaluate the selectivity of the proposed detecting method, its performance on formaldehyde fast detection with the coexistence of 2 ppm of other main indoor pollutants (benzene, toluene, methanol and ethanol) were investigated. A series of exposure time (5 min, 10 min, 15 min and 20 min) were chosen due to heating at 75 °C, the optimized condition measured at room temperature (5 min) for formaldehyde detection may be inapplicable. As shown in Fig. 6, after exposure to 2 ppm of formaldehyde for 5 min with the presence of 2 ppm of toluene, benzene, methanol or ethanol, the PL intensity of ZIF-8(b) was little influenced by these interferent substances. The similar phenomenon was observed with the exposure time prolonging to 10 min, 15 min and 20 min, which suggests that the present sensing platform exhibits good selectivity and feasibility for the detection of indoor formaldehyde.

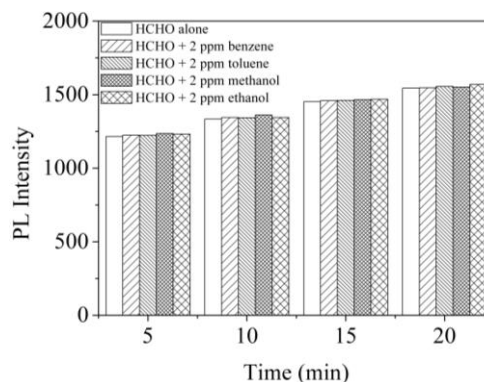


Fig. 6 Comparison of Solid-state photoluminescence intensity of the guest-free phase ZIF-8(b) after exposure to 2 ppm formaldehyde in the absence and presence of other main indoor pollutants (benzene, toluene, methanol and ethanol) with a concentration of 2 ppm in various time (5 min, 10 min, 15 min and 20 min). $\lambda_{\text{ex}} = 350$ nm, $\lambda_{\text{em}} = 410$ nm.

3.6. Detection mechanism

To explain the detection mechanism, the luminescent mechanism of ZIF-8 was deduced first by investigating the solid-state PL excitation spectra of the neutral ligand 2-methylimidazole and the as-synthesized ZIF-8(a) at room temperature. A series of emission wavelengths were chosen for this purpose. As shown in the Fig. 7a, the neutral ligand 2-methylimidazole exhibited its strongest PL intensity at 360 nm emission wavelength with the excitation wavelength of 310 nm, which is possibly attributed to the $\pi^* - \pi$ transition of 2-methylimidazole.²⁶⁻³¹ While, the as-synthesized ZIF-8(a) was found to exhibit its strongest PL emission intensity at 380 nm

with the excitation wavelength at 350 nm (Fig. 7b), which is totally different with that of neutral ligand 2-methylimidazole. According to the previous reports, when one of the composite fractions of MOFs is transition-metal ions without unpaired electrons, especially those having d^{10} configurations (such as Zn^{2+} , Cu^{2+} and Cd^{2+}), they can highly yield linker-based emissive.³¹⁻³⁵ Therefore, it is reasonable to deduce that the luminescent of ZIF-8 is based on linker-based emission. The red shift 20 nm of emission wavelength compared to the neutral ligand 2-methylimidazole is owing to the coordination of 2-methylimidazole to the Zn^{2+} .

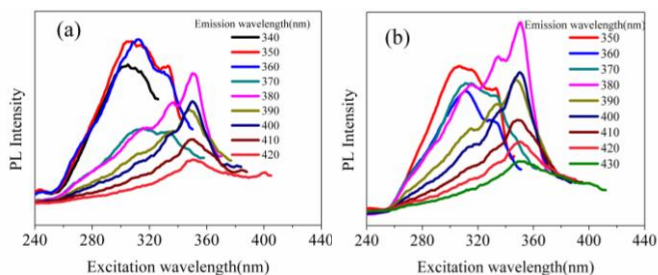


Fig. 7 (a) The excitation spectra of 2-methylimidazole under different emission wavelengths. (b) The excitation spectra of as-synthesized ZIF-8(a) under different emission wavelengths.

In order to explain the possible mechanism of the “turn-on” effect of formaldehyde on the PL emission intensity, SEM and XRD analysis of ZIF-8(b) were operated to compare the morphology changes after exposure to formaldehyde gas and air for 1 h, respectively. Results indicated that there were obvious changes in the morphology of ZIF-8(b): the particles agglomerated after exposure to 20 ppm of formaldehyde for 1 h (Fig. 8a and 8b), illustrating the specific interaction between formaldehyde and host framework. But the basic 3D structure of host framework was still maintained, which shows the good stability of ZIF-8 as testified by XRD data as well (Fig. 8c). Meanwhile, FT-IR spectra of the guest-free phase ZIF-8(b) were carried out after exposure to air and 20 ppm formaldehyde for 1 h, respectively. As shown in Fig. 8d, taking the two curves into comparison, a weak absorption band in the region of $1620 - 1640\text{ cm}^{-1}$ was observed in the spectrum of the guest-free phase ZIF-8(b) after exposure to formaldehyde at room temperature, indicating the existence of C=O stretching vibrations. The existence of C=O stretching vibrations meant that the existence of formaldehyde gas in ZIF-8 interacting with the host frameworks of ZIF-8, which enhanced the structural rigidity of MOFs and influenced the luminescent characterization based on linker-based emission. The principle of the strategy is illustrated in Scheme 1.

The reason for the little influence of benzene or toluene on PL intensity of ZIF-8(b) exposing to formaldehyde was mainly attributed to their larger kinetic diameter (k_D , 6.8 \AA and 6.7 \AA , respectively), which is almost twice larger than the pore window of ZIF-8 (3.4 \AA), preventing them from getting into the pore and interacting with the host frameworks of ZIF-8. While, as for methanol and ethanol, whose kinetic diameters are

similar with formaldehyde, played little effect on the PL emission intensity of ZIF-8 was due to the weak interaction of their functional group ($-OH$) with the host framework of ZIF-8.

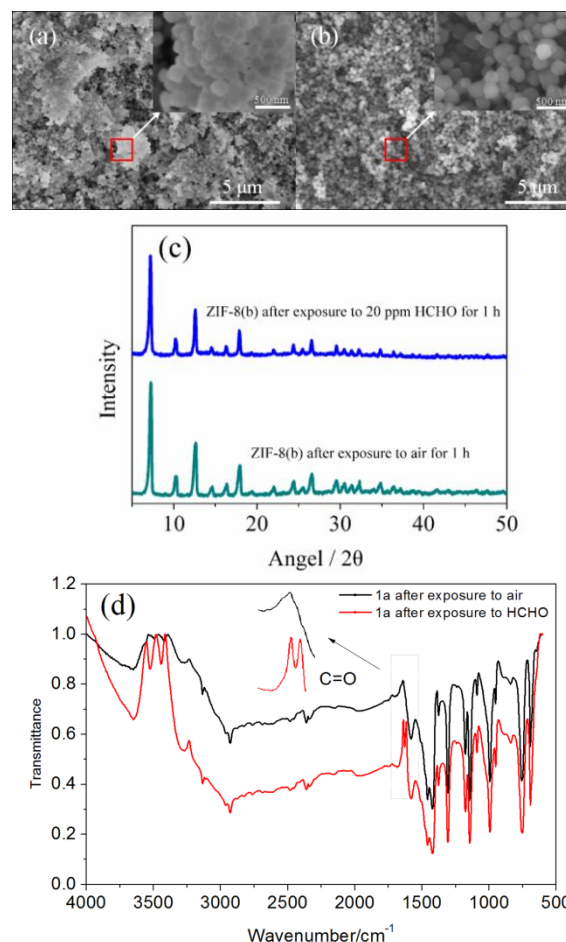
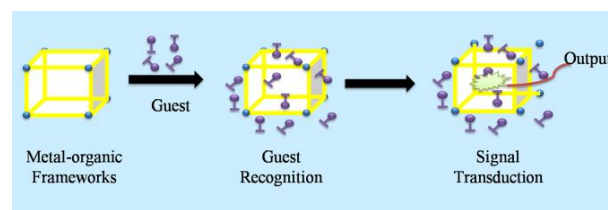


Fig. 8 (a) SEM picture of ZIF-8(b) after exposure to 20 ppm formaldehyde for 1 h. The upper-right corner figure represents an enlarged view of the red square area. (b) SEM picture of ZIF-8(b) after exposure to air for 1 h. The upper-right corner figure represents an enlarged view of the red square area. (c) XRD patterns of ZIF-8(b) after exposure to 20 ppm formaldehyde and air for 1 h, respectively. (d) FT-IR spectra of samples. Red and black data correspond to ZIF-8(b) after exposure to 20 ppm formaldehyde and air for 1 h, respectively.



Scheme 1. A possible signal transduction strategy in the inner of Metal-organic frameworks based on the specific interaction between guest and host frameworks is presented.

4. Conclusion

In summary, a rapid, convenient and highly sensitive ZIF-8-based sensor is presented for PL “turn-on” detection of indoor formaldehyde. On the basis of the PL enhancement of ZIF-8 by gaseous formaldehyde, the sensor exhibits high sensitivity,

good reproducibility and selectivity. Moreover, we also elaborate the enhancement of PL emission intensity is most possibility due to the specific interaction of HCHO with the host framework of ZIF-8. The enhancement mechanism was explored by means of some characterization based on the agglomeration of material itself and the appearance of C=O in the host framework which may lead to the structural rigidity enhancement of MOFs. Taking good performance of ZIF-8-based luminescent sensor, it is expected that by synthesizing more specific MOFs, highly sensitive sensor based host-guest strategy may be applied to the detection of a wide range of gaseous pollutants.

Acknowledgements

This work was supported by the National Nature Science Foundation of China (No. 21277016), the Research Project of Chinese Ministry of Education (No113017A), and program for Changjiang Scholars and Innovative Research Team in University (IRT_13R05).

Notes and references

Key Laboratory of Industrial Ecology and Environmental Engineering (Ministry of Education, China), School of Environmental Science and Technology, Dalian University of Technology, Dalian, 116024, China. Fax: +86-411-84706263; Tel: +86-411-84706263; E-mail address: zhaohuim@dlut.edu.cn;

- Y.-L. Li, S. Yin and B.-Y. Huang, *J. Foshan Univ. Natural Science Edition*, 2003, **49**, 52-74.
- D. W. Cockcroft, V. H. Hoepfner and J. Dolovich, *CHEST*, 1982, **82**, 49-53.
- V. J. Cogliano, Y. Grosse, R. A. Baan, K. Straif, M. B. Secretan and F. E. Ghisssassi, *ENVIRON HEALTH PERSP*, 2005, **113**, 1205-1208.
- K. J. Lee, N. Shiratori, G. H. Lee, J. Miyawaki, I. Mochida, S.-H. Yoon and J. Jang, *Carbon*, 2010, **48**, 4248-4255.
- S. J. Armour, *International Task Force 40: Toxic Industrial Chemicals(TICs) Operational and Medical Concerns*, U.S. Government Printing Office: Washington, DC, 2001.
- WHO Air Quality Guidelines for Europe*, 2nd ed.; World Health Organization: Copenhagen, 2000.
- R. Pal and K. H. Kim, *J. Sep. Sci*, 2007, **30**, 2708-2718.
- G. Ferey, *Chem. Soc. Rev.*, 2008, **37**, 191-214.
- H. Li, M. Eddaoudi, M. O'Keeffe and O. M. Yaghi, *Nature*, 1999, **402**, 276-279.
- H. Deng, C. J. Doonan, H. Furukawa, R. B. Ferreira, J. Towne, C. B. Knobler, B. Wang and O. M. Yaghi, *Science*, 2010, **327**, 846-850.
- M. O'Keeffe and O. M. Yaghi, *Chem. Rev.*, 2012, **112**, 675-702.
- Y.-W. Li, J.-R. Li, L.-F. Wang, B.-Y. Zhou, Q. Chen and X.-H. Bu, *J. Mater. Chem. A.*, 2013, **1**, 495-499.
- J.-M. Zhou, W. Shi, N. Xu and P. Cheng, *Inorg. Chem.*, 2013, **52**, 8082-8090.
- Z.-Z. Lu, R. Zhang, Y.-Z. Li, Z.-J. Guo and H.-G. Zheng, *J. Am. Chem. Soc.*, 2011, **133**, 4172-4174.
- D. Tian, Y. Li, R.-Y. Chen, Z. Chang, G.-Y. Wang and X.-H. Bu, *J. Mater. Chem. A.*, 2014, **2**, 1465-1470.
- N. B. Shustova, A. F. Cozzolino, S. Reineke, M. Baldo and M. Dinca, *J. Am. Chem. Soc.*, 2013, **135**, 13326-13329.
- J. An, C. M. Shade, D. A. Chengelis-Czegan, S. Petoud and N. L. Rosi, *J. Am. Chem. Soc.*, 2011, **133**, 1220-1223.
- J.-M. Zhou, W. Shi, N. Xu, and P. Cheng, *Inorg. Chem.*, 2013, **52**, 8082-8090.
- Y. Yu, X.-M. Zhang, J.-P. Ma, Q.-K. Liu, P. Wang and Y.-B. Dong, *Chem Commun*, 2014, **50**, 1444-1446.
- K. S. Park, Z. Ni, A. P. C \acute{a} J. Y. Choi, R. Huang, F. J. Uribe-Romo, H. K. Chae, M. O'Keeffe and O. M. Yaghi, *Proc. Natl. Acad. Sci. U.S.A.*, 2006, **103**, 10186-10191.
- J. C. Tan, T. D. Bennett and A. K. Cheetham, *Proc. Natl. Acad. Sci. U.S.A.*, 2010, **107**, 9938-9943.
- N. Chang, Z.-Y. Gu and X.-P. Yan, *J. Am. Chem. Soc.*, 2010, **132**, 13645-13647.
- S. Tanaka, K. Kida, M. Okita, Y. Ito and Y. Miyake, *Chem. Lett.*, 2012, **41**, 1337-1339.
- A. F. Gross, E. Sherman and J. J. Vajo, *Dalton Trans*, 2012, **41**, 5458-5460.
- M. He, J. Yao, Q. Liu, K. Wang, F. Chen and H. Wang, *Microporous Mesoporous Mater.*, 2014, **184**, 55-60.
- T. Jiang, Y.-F. Zhao and X.-M. Zhang, *Inorg. Chem. Commun.*, 2007, **10**, 1194-1197.
- G. Tian, G. Zhu, Q. Fang, X. Guo, M. Xue, J. Sun and S. Qiu, *J. Mol. Struct.*, 2006, **787**, 45-49.
- X. Shi, G. Zhu, Q. Fang, G. Wu, G. Tian, R. Wang, D. Zhang, M. Xue and S. Qiu, *Eur. J. Inorg. Chem.*, 2004, **2004**, 185-191.
- S.-L. Zheng, J.-H. Yang, X.-L. Yu, X.-M. Chen and W.-T. Wong, *Inorg. Chem.*, 2003, **43**, 830-838.
- H.-Y. Bai, J.-F. Ma, J. Yang, L.-P. Zhang, J.-C. Ma and Y.-Y. Liu, *Cryst. Growth Des.*, 2010, **10**, 1946-1959.
- H.-Y. Bai, J.-F. Ma, J. Yang, Y.-Y. Liu, W. Hua and J.-C. Ma, *Cryst. Growth Des.*, 2010, **10**, 995-1016.
- Q.-R. Fang, G.-S. Zhu, M. Xue, J.-Y. Sun, F.-X. Sun and S.-L. Qiu, *Inorg. Chem.*, 2006, **45**, 3582-3587.
- C. A. Bauer, T. V. Timofeeva, T. B. Settersten, B. D. Patterson, V. H. Liu, B. A. Simmons and M. D. Allendorf, *J. Am. Chem. Soc.*, 2007, **129**, 7136-7144.
- E.-C. Yang, H.-K. Zhao, B. Ding, X.-G. Wang and X.-J. Zhao, *Cryst. Growth Des.*, 2007, **7**, 2009-2015.
- G.-H. Wang, Z.-G. Li, H.-Q. Jia, N.-H. Hu and J.-W. Xu, *CrystEngComm*, 2009, **11**, 292-297.
- H.-J. Liu, X.-T. Tao, J.-X. Yang, Y.-X. Yan, Y. Ren, H.-P. Zhao, Q. Xin, W.-T. Yu and M.-H. Jiang, *Cryst. Growth Des.*, 2008, **8**, 259-264.